



1 Are seamounts refuge areas for fauna from polymetallic  
2 nodule fields?

3 Daphne Cuvelier<sup>1\*</sup>, Pedro A. Ribeiro<sup>1,2\*</sup>, Sofia P. Ramalho<sup>1,3\*</sup>, Daniel Kersken<sup>4,5</sup>, Pedro Martinez  
4 Arbizu<sup>5</sup>, Ana Colaço<sup>1</sup>

5 <sup>1</sup> MARE – Marine and environmental sciences centre/IMAR – Instituto do Mar/Centro OKEANOS –  
6 Universidade dos Açores, Rua Prof. Dr. Frederico Machado 4, 9901-862 Horta, Portugal

7 <sup>2</sup> Current address: Department of Biological Sciences and K.G. Jebsen Centre for Deep-Sea Research,  
8 University of Bergen, Bergen, Norway.

9 <sup>3</sup> Current address: Departamento de Biologia & CESAM, Universidade de Aveiro, Campus  
10 Universitário de Santiago, 3810-193 Aveiro, Portugal

11 <sup>4</sup> Department of Marine Zoology, Senckenberg Research Institute and Natural History Museum,  
12 Senckenberganlage 25, 60325 Frankfurt am Main, Germany

13 <sup>5</sup> German Centre for Marine Biodiversity Research (DZMB), Senckenberg am Meer, Südstrand 44,  
14 26382 Wilhelmshaven, Germany

15 \* Contributed equally to this work/Corresponding authors: Daphne Cuvelier  
16 ([daphne.cuvelier@gmail.com](mailto:daphne.cuvelier@gmail.com)), Pedro Ribeiro ([Pedro.Ribeiro@uib.no](mailto:Pedro.Ribeiro@uib.no)) and Sofia Pinto Ramalho  
17 ([sofia.pinto.ramalho@gmail.com](mailto:sofia.pinto.ramalho@gmail.com))

18 Running title: Seamounts as refuge areas for nodule fauna

19 Six keywords: megafauna, seamounts, nodule fields, image analysis, deep sea, mining

20 Abstract

21 Seamounts are abundant and prominent features on the deep-sea floor and intersperse with the  
22 nodule fields of the Clarion-Clipperton Fracture Zone (CCZ). There is a particular interest in  
23 characterising the fauna inhabiting seamounts in the CCZ because they are the only other ecosystem  
24 in the region to provide hard substrata besides the abundant nodules on the soft sediment abyssal  
25 plains. It has been hypothesised that seamounts could provide refuge for organisms during deep-sea  
26 mining actions or that they could play a role in the (re-)colonisation of the disturbed nodule fields.  
27 This hypothesis is tested by analysing video transects in both ecosystems, assessing megafauna  
28 composition and abundance.

29 Nine video transects (ROV dives) from two different license areas and one Area of Particular  
30 Environmental Interest in the eastern CCZ were analysed. Four of these transects were carried out as  
31 exploratory dives on four different seamounts in order to gain first insights in megafauna  
32 composition. The five other dives were carried out in the neighbouring nodule fields in the same  
33 areas. Variation in community composition observed among and along the video transects was high,  
34 with little morphospecies overlap on intra-ecosystem transects. Despite these observations of  
35 considerable faunal variations within each ecosystem, differences between seamounts and nodule  
36 fields prevailed, showing significantly different species associations characterising them, thus  
37 questioning their use as a possible refuge area.



## 38 1. Introduction

39 Seamounts are abundant and prominent features on the deep-sea floor (Wessel et al., 2010). They  
40 are common in all the world's oceans, occurring in higher abundances around mid-ocean ridges,  
41 island-arc convergent areas, and above upwelling mantle plumes (Kitchingman et al., 2007).  
42 Seamounts are generally isolated, typically cone shaped undersea mountains rising relatively steeply  
43 at least several hundred meters from the deep-sea floor. Seamounts comprise a unique deep-sea  
44 environment, characterised by substantially enhanced currents and a fauna that is dominated by  
45 suspension feeders, such as corals (Rogers, 2018). They represent hard substrata in the otherwise  
46 soft sediment deep sea and can thus be considered habitat islands (Beaulieu, 2001). Given the  
47 growing evidence that seamounts differ substantially across a range of spatial scales, the concept of  
48 seamounts as a single, relatively well-defined habitat type is outdated (Clark et al., 2012). Depth and  
49 substrate type are key elements in determining the composition and distribution of benthic fauna on  
50 seamounts, while location is likely the subsequent most important driver of faunal composition and  
51 distribution patterns (e.g. Tittensor et al., 2009). Connectivity varies substantially between  
52 seamounts, resulting in the presence of taxa with very localised to very wide distributions (Clark et  
53 al., 2010).

54  
55 The Clarion-Clipperton Fracture Zone (CCZ), in the equatorial eastern Pacific Ocean, is most known  
56 for its extensive polymetallic nodule fields that will potentially be mined in the future. In this area,  
57 nodules represent the most common hard substrate on the soft-sediment abyssal plains, and many  
58 organisms rely on them for survival (Vanreusel et al., 2016). Removal of hard substrate through  
59 mining actions will impact all these organisms, which were estimated at about 50% of all megafaunal  
60 species in the CCZ (Amon et al., 2016). Nodule fields in the CCZ are interspersed by seamounts  
61 (Wedding et al., 2013), the only feature offering hard substrata besides the nodules. Based on this  
62 feature/characteristic, it has been hypothesised that seamounts could provide refuge for organisms  
63 during deep-sea mining activities or that seamounts could play a role in the (re-)colonisation of the  
64 disturbed nodule fields. Whether or not this is true may have important implications for  
65 management of the impacts of polymetallic nodule mining in the CCZ. However, knowledge on the  
66 biodiversity inhabiting seamounts in this region is currently lacking.

67 The objectives of the current study were twofold: (i) Provide first insights in seamount megafauna  
68 within the CCZ, (ii) Compare the benthic fauna inhabiting seamounts and nodule fields in the eastern  
69 CCZ. Since this is the first time the seamounts at the eastern CCZ were visited, a separate section is  
70 dedicated to describe these first insights.

## 71 2. Material and Methods

### 72 2.1. Study site and data

73 During the SO239 ECORESPONSE cruise (Martinez Arbizu and Haeckel, 2015), four seamounts were  
74 visited for the first time within two different license areas and one area of particular environmental  
75 interest (APEI) within the Clarion-Clipperton Fracture zone (CCZ) (Table 1). Nodule fields within the  
76 same license areas were visited and sampled as well. Video imagery and faunal samples were  
77 collected by a Remotely Operated Vehicle (ROV Kiel 6000 (GEOMAR), equipped with a high  
78 definition Kongsberg OE14-500 camera).



79 Seamount transects were carried out uphill towards the summit resulting in a depth gradient along  
80 the transect, whilst nodule transects featured rather stable depth ranges (Table 1). The four  
81 seamount transects were characterised by different depth ranges and lengths but were all situated  
82 on the north to north-western flanks of the seamounts (Table 1 and Fig. S1). The names of the  
83 seamounts used here, Rüppel and Senckenberg (BGR, German License area), Heip (GSR, Belgian  
84 License area) and Mann Borgese (APEI3), are the ones agreed upon by the scientist during the  
85 ECORESPONSE cruise (Martinez Arbizu and Haeckel, 2015), pending incorporation of these names in  
86 the GEBCO gazetteer. The seamounts differed in shape and size with Senckenberg and Heip being a  
87 sea-mountain range, while Rüppel and Mann Borgese were more isolated, stand-alone seamounts  
88 (Fig. S1). Nodule field dives were carried out on relatively flat surfaces (maximum depth range  
89 covered during a dive or transect was 30m difference, Table 1) and were referred to by the dive  
90 number and license area. The five nodule transects were all located between 4000-5000m depth and  
91 the transects differed in length between dives as well (Table 1). Within the same license area  
92 distance between different transects was 16 to 60km, while distance between license areas added  
93 up to several hundreds of kilometres (minimum ~700kms BGR – GSR, Fig. 1).

94 Investigated areas were restricted to the eastern part of the CCZ with APEI3 being the most north-  
95 and westward bound area. The optical resolution of the camera enabled reliable identification of  
96 organisms larger than 3 cm (Martinez Arbizu and Haeckel, 2015). The combination of exploration  
97 and opportunistic sampling restricted a systematic image collection. ROV travelling altitude, speed  
98 and camera zoom were kept constant whenever possible, while pan and tilt of the ROV camera were  
99 not.

## 100 2.2. Video analysis and statistics

101 All videos were annotated to the lowest taxonomic level possible. The number of morphospecies,  
102 defined as morphologically different organisms within the lowest taxonomic group identified, were  
103 assessed. Identifications were double checked with scientists working in the same area as well as  
104 taxonomic experts and comprise different taxonomic levels (e.g. Genus, Family). Those ID's  
105 restricted to higher taxon groups (Family, Class, etc.) and for which it was impossible to attribute a  
106 morphospecies, are referred to as taxa and are likely to morphologically differ between transects.  
107 Xenophyophores, living on the soft sediment deep-sea floor, were less prominently present at  
108 seamounts than at nodule fields and were not quantified. Fish (Actinopterygii), crustaceans  
109 (Nematocarinidae, Aristeidae, Peracarida) and Polychaeta were quantified but left out of the  
110 comparing analysis due to their lack of representativity and possible attraction due to ROV lights.  
111 The same was done for jellyfish and other doubtful ID's that could not be confidently assigned to a  
112 higher taxonomic group (Table A1).

113 ROV transects on the seamounts were carried out as exploratory dives. Sampling strategy both at  
114 seamounts and nodule fields combined video and sampling or specimen collection. Due to varying  
115 altitude of the ROV and the use of camera pan, tilt and zoom, it was not possible to use surface  
116 coverage as a standardisation measure. We used video transect length instead. Faunal densities  
117 were calculated as the number of observations per 100m, in order to compensate for time spent  
118 collecting samples and differing transect lengths. Statistical testing was carried out in R (R core team,  
119 2018) and the Non-metric multidimensional scaling analysis (NMDS) was based on Bray-Curtis  
120 dissimilarity and used the vegan package (Oksanen et al., 2018).  
121



## 122 3. Results

123 A total of 252 taxa were observed across the two adjacent ecosystems, of which 207 (or 82%) could  
124 be identified to a morphospecies level. At a first view, morphospecies revealed to be quite different  
125 between seamounts and nodule fields (Fig. 2). While the number of faunal observations at the  
126 seamount transects were within similar ranges (33.1-40.7 ind./100m), those at the nodule transects  
127 featured both highest and lowest values (7.59-89.23 ind./100m) (Table 1). The lowest number of  
128 faunal observations were done at the two APEI3 nodule transects (ROV13 and 14) and highest at the  
129 GSR nodule transect ROV08. What follows is a first description of eastern CCZ seamount megafauna  
130 (3.1.) and a detailed comparison with the neighbouring nodule fields (3.2.)

### 131 3.1. Insights in CCZ seamount megafauna

132 The most abundant and diverse (most morphospecies) taxa at the seamount transects comprised  
133 Echinodermata (Asteroidea, Crinoidea, Holothuroidea and Ophiuroidea), Anthozoa (Actiniaria,  
134 Alcyonacea, Pennatulacea, Scleractinia) and Porifera (Hexactinellida) (Table A1, Fig. 3). Keeping in  
135 mind the limitation of the video sampling, differences among the benthic seamount community  
136 composition are described here.

137 The transect at Mann Borgese (APEI3) was characterised by high densities of Antipatharia, more  
138 specifically Antipathidae (19.11 ind./100m), and solitary Scleractinia (8.11 ind./100m) (Table A1, Fig.  
139 3). Antipathidae observations were mostly grouped at the end of the video transect, i.e. at the  
140 summit. Densities of both Antipatharia and Scleractinia were much lower on the other seamount  
141 transects ( $\leq 0.2$  ind./100m) with Scleractinia being absent from Heip and Senckenberg transects.  
142 Alcyonacea corals were observed on all seamount transects. Isididae were found at Senckenberg and  
143 Heip transects, and one individual from Chrysogorgiidae was observed at the latter as well. Varying  
144 numbers of Primnoidae were observed on all transects (Table A1). High abundances of Pennatulacea  
145 were observed at Senckenberg (3.64 ind./100m), representing about 26% of sessile fauna  
146 annotations for this transect.

147 Enteropneusta were only observed on Rüppel and Senckenberg transects in the BGR area,  
148 represented by two different morphospecies, namely *Yoda* morphospecies (Torquaratoridae) at  
149 Rüppel and *Saxipendium* morphospecies (Harrimaniidae) at Senckenberg.

150 Highest Polychaeta densities were observed at Heip transect in the GSR area (4.2 ind./100m vs. 0.56  
151 and 0.32 ind./100m in BGR and 0.11 ind./100m in APEI3). Free-swimming Acrocirridae were  
152 observed in very high densities as well (Table A1). Aphroditidae polychaetes were only present at  
153 the BGR transects (3 ind. at Rüppel and 1 at Senckenberg) (Table A1).

154 Porifera densities were highest at the Heip transect (3 ind./100m), followed by Rüppel (2.72  
155 ind./100m), Senckenberg (1.92 ind./100m) and lastly Mann Borgese (0.68 ind./100m). Six Porifera  
156 families were annotated featuring >7 to >10 morphospecies (Fig. 3, Table A1). Cladorhizidae (two  
157 individuals) were only observed on Heip transect, and one *Poliopogon* sp. (Phoronematidae) was  
158 observed at Mann Borgese transect. Rossellidae gen. sp. nov. was present on three seamount  
159 transects, exception being Mann Borgese.



160 Overall Echinodermata densities were highest at Senckenberg seamount (17.64 ind./100m),  
161 followed by Rüppel (12.24 ind./100m) (Table A1, Fig. 3), both adding up to 60% of all image  
162 annotations for these transects. The number of morphospecies for all echinoderm taxa (Asteroidea,  
163 Echinoidea, Holothuroidea and Crinoidea) was also highest at these 2 seamounts in the BGR area  
164 (Fig. 3). For comparison, echinoderms at Heip (11.68 ind./100m) and Mann Borgese transects (3.08  
165 ind./100m) were responsible for 49% and 8.8% of observations respectively. Crinoid densities were  
166 highest at Senckenberg (4.32 ind./100m), while Holothuroidea were most abundant at Rüppel (5.2  
167 ind./100m). The holothuroid families of Elpidiidae and Laetmogonidae were only observed at  
168 Senckenberg and Rüppel (BGR). Psychropotid and synallactid holothuroids were observed on all  
169 seamounts, represented by different morphospecies. Deimatid holothuroids were not observed on  
170 Mann Borgese, but were present in the three other seamount transects, again with different  
171 morphospecies and densities. Velatid Asteroidea were only observed at Senckenberg and Rüppel  
172 (BGR), while Brisingida and Paxillosida were observed on all four seamounts. Aspidodiadematid  
173 echinoids were absent from the Heip transect and urchinid echinoids were absent from the Mann  
174 Borgese transect.

175 A species accumulation curve (Fig. 4a) confirmed the limitations of the restricted and exploratory  
176 nature of the sampling as no asymptote was reached. The rarefaction curves (Fig. 4b) showed that  
177 the transects with the most faunal observations, which corresponded here to the longer transects,  
178 were more diverse. However, at smaller sample sizes curves did not cross, thus maintaining the  
179 differences observed at higher sample sizes with the Senckenberg transect (ROV04) most diverse  
180 followed by Rüppel (ROV02) (both BGR). The video transect carried out at Mann Borgese (ROV15,  
181 APE13) was the least diverse.

182 A comparison of all morphospecies observed along the 4 transects was presented in a Venn diagram  
183 (Fig. 5a). Each seamount transect was characterised by a highest number of unique morphospecies,  
184 only observed on the transect in question and not elsewhere. Only two morphospecies were present  
185 in all seamount transects, namely a small red galatheid crab and a foliose sponge. Highest number of  
186 overlapping morphospecies (#14) was observed between Rüppel and Senckenberg, both in the BGR  
187 area (Fig. 5a). Mann Borgese showed the smallest degree of overlap with the other transects (Fig.  
188 5a).

189 Due to the limited sample size, the representativity of the observed biological patterns remains to  
190 be corroborated by a more elaborate sampling strategy.

### 191 3.2. Comparison of seamount and nodule field faunal composition and variation

192 The faunal composition and richness (number of morphospecies in higher taxonomic groups) of the  
193 nodule transects can be consulted in Fig. 3 and Table A1. In concordance with the seamount  
194 transect, the species accumulation curve of the nodule transects did not reach an asymptote either  
195 (Fig. 4c). The rarefaction curves showed that the relations among transects were less linear for the  
196 nodule transects versus the seamount ones and did cross at smaller sample sizes (Fig. 4d). ROV13  
197 and ROV14 transects (both APE13) were the longest in distance travelled (Table 1) but featured less  
198 faunal observations. At small sample sizes, the richness at ROV13 and 14 was highest. ROV08 and  
199 ROV10 (both GSR) showed parallel curves with ROV08 being more diverse (Fig. 4d).



200 A venn diagram showing the morphospecies overlap among the nodule transects showed a total of 5  
201 species re-occurring on all 5 transects (Fig. 5b). These were: Munnopsidae msp. 1 (Isopoda,  
202 Crustacea), Actiniaria msp.7 (Cnidaria), Ophiuroidea msp. 6 (Echinodermata), *Holascus* sp and  
203 *Hyalonema* sp. (Hexactinellida, Porifera). There was a high number of unique morphospecies for  
204 each transect, though not as high as for the seamount transects (Fig. 5). ROV13 and 14 (both APEI3)  
205 showed littlest overlap with the other transects, which is similar to what was observed at the  
206 seamounts.

207 Observations and quantifications of morphospecies confirmed the high degree of dissimilarity  
208 between the two neighbouring ecosystems. Porifera, Ophiuroidea (Echinodermata), Actiniaria and  
209 Alcyonacea (Cnidaria) were more abundant at nodule fields (Fig. 3). These taxonomic groups were  
210 also most diverse on nodule fields (i.e. highest number of morphospecies), exception being the  
211 Alcyonacea which featured more morphospecies on the seamounts (12 to 8 morphospecies for  
212 seamounts and nodule fields respectively) (Fig. 3). Of all Porifera, Cladhorizidae were more diverse  
213 at nodule fields than at seamounts (7 to 1 morphospecies, respectively).

214 There were only 21 morphospecies (10%) that were observed both on seamounts and nodule fields  
215 (Fig. 6). While this subset of morphospecies occurred in both ecosystems, they did so in very  
216 different densities, i.e. very abundant in one ecosystem and very low in abundance in the other,  
217 examples are Galatheidae small red msp. (Decapoda, Crustacea), *Synallactes white* msp.  
218 (Holothuroidea), Ophiuroidea msp. 5 and 6, Comatulida msp. 1 (Crinoidea), *Hyalonema* sp. and  
219 *Hyalostylus* sp. (both Hexactinellida, Porifera) (Fig. 6).

220 Three Ophiuroid morphospecies were present at both seamounts and nodule fields (Fig. 8). The  
221 majority of the very abundant ophiuroids observed at the CCZ seamounts were small and situated  
222 on hard substrata (morphospecies 5). While the most abundant morphospecies at nodule fields  
223 (morphospecies 6) was mostly observed on the soft sediments of the nodule transects. This  
224 morphospecies was only rarely observed on the seamounts (Fig. 3). Another easily recognisable  
225 morphospecies was found on Porifera, corals and animal stalks and was more abundant at  
226 seamounts than at nodule fields (morphospecies 4) (Fig. 2 and 3).

227 Crinoidea, Asteroidea (both Echinodermata) and Antipatharia (Cnidaria) were more abundant on the  
228 seamounts. This coincided with a higher diversity for Asteroidea and Antipatharia on the seamounts  
229 as well. Crinoidea diversity was similar (5 to 4 morphospecies comparing seamounts to nodule  
230 fields). Holothuroidea occurred in similar densities in both ecosystems, though they were  
231 characterised by different morphospecies (Fig. 3). Overall densities of Echinoidea were highest at  
232 nodule fields, though this was mostly due to one very abundant morphospecies, namely  
233 Aspidodiadematidae msp 1 (Fig. 3). Besides this one very abundant morphospecies, which was only  
234 present at nodule fields, echinoids showed higher densities at seamounts and were more diverse (11  
235 morphospecies vs. 5 at nodule fields).

236 There was no morphospecies overlap for Tunicata, Antipatharia, and Actiniaria. Alcyonacea,  
237 Ceriantharia, Corallimorphidae and Crinoidea only shared 1 morphospecies between seamounts and  
238 nodule fields, namely *Callozostron cf. bayeri*, Ceriantharia msp. 2, *Corallimorphus* msp. 2 and  
239 Comatulida msp. 1 respectively (Fig. 6).



240 There were no observations of Enteropneusta, Scleractinia and Zoantharia (Cnidaria), Aphroditidae  
241 (Polychaeta) or holothuroid Deimatidae at the nodule fields transects (Table A1). While  
242 Actinopterygii were left out of the analysis, it should be noted that fish observations were more  
243 abundant and diverse at the seamounts than on the nodule fields (Table A1).

244 There was quite some faunal variation observed along the video transects carried out in the  
245 different license areas, both for seamounts and nodule fields (see fig. 5). The (dis)similarities were  
246 analysed by a nMDS analysis, which grouped the 9 different video transects based on their taxonomic  
247 composition. Despite the large intra-ecosystem variation, they pooled in two distinct groups  
248 separating the nodule fields from the seamounts (Fig. 7a). Within each group, BSR and GSR transects  
249 were more similar to one another both for seamounts and nodule fields, whilst APEI3 transects  
250 stood out more.

251 The Kendall's coefficient of concordance (W, Legendre, 2005) corroborated the existence of two  
252 significantly different species associations, whose composition corresponded to the fauna  
253 characterising the nodule fields ( $W=0.20$ ,  $p<0.001$ , after 999 permutations) and the seamounts  
254 ( $W=0.30$ ,  $p<0.001$ , after 999 permutations).

255 Depth was fitted as a vector on top of the nMDS plot (Fig. 7b) and showed that the discrepancy in  
256 faunal composition between the two ecosystems also corresponded to a difference in depth, with  
257 the nodule transects all being situated below the 4000m isobath and the seamount transects ranging  
258 from 1650 to >3500m (Fig. 7b).

## 259 4. Discussion

### 260 4.1. Intra-ecosystem faunal variation

261 Community composition varied markedly within seamounts and nodule fields. The limited sampling  
262 ( $n=9$  transects), across different localities and for the seamounts different depth gradients,  
263 precluded any general conclusions on quantifications of biodiversity *per se*. However, taking this into  
264 account, it was also the first time seamounts were visited in the area, thus granting first insights in  
265 the fauna inhabiting these seamounts and allowing a first comparison with nodule faunal  
266 composition.

267 The two BGR seamount video transects were geographically closest to each other and were most  
268 similar in faunal composition but also in depth. For seamounts, distance separating them might be a  
269 less determining factor since adjacent seamounts were shown to be very different in inhabiting  
270 fauna (Schlacher et al., 2014; Boschen et al., 2015). Overall, parameters that vary with depth are  
271 considered major drivers of species composition on seamounts (Clark et al., 2010; McClain et al.,  
272 2010). Depth could be explanatory for the higher degree of similarity of these two BGR seamount  
273 transects and, to a lesser extent, the Heip seamount transect (GSR). Similarly, it could explain the  
274 higher dissimilarity with Mann Borgese (APEI3) who featured the shallowest transect and summit,  
275 which was dominated by Antipatharia. Antipatharians were previously reported to be more  
276 dominant towards peaks as compared to mid-slopes at corresponding depths (Genin et al., 1986).  
277 Based on their filter-feeding strategy, Porifera (except carnivorous Cladorhizidae), were also thought  
278 to benefit from elevated topography (peaks) or exposed substrata in analogy to corals (Genin et al.,  
279 1986; Clark et al., 2010), though no such pattern was apparent here. Porifera are notoriously difficult  
280 to identify based on imagery. Although the sampled individuals allowed some identifications to  
281 genus or species level (Kersken et al., 2018a and b), identifications remained hard to extrapolate



282 across the different video transects. Generally, as in our study, seamount summits have been more  
283 intensively sampled (Stocks, 2009) although the little work done at seamount bases and deep slopes  
284 indicated that these areas support distinct assemblages (Baco, 2007).

285 Among the nodule transects a considerable amount of variation in faunal composition was observed  
286 (this study, Vanreusel et al., 2016). The two APEI3 nodule transects (ROV13 and 14) stood out, both  
287 in the low number of faunal observations, faunal composition and diversity. They were also the only  
288 two transects situated below the 4500m isobaths. But rather than depth, the nodule coverage was  
289 thought to be more of a driving factor, since the density of nodule megafauna was shown to vary  
290 with nodule size and density/coverage (Stoyanova, 2012; Vanreusel et al., 2016, Simon-Llédó et al.,  
291 2019). Here as well, the APEI3 transects were characterised by a high nodule coverage (~40-88%,  
292 Vanreusel et al., 2016), whereas the BGR and GSR nodule transects (ROV3 and ROV 8 + 10,  
293 respectively) had a nodule coverage <30% and were more similar in faunal composition (Vanreusel  
294 et al., 2016). The more oligotrophic surface waters of the northern CCZ were proposed to be the  
295 cause of the overall lower densities at APEI3 nodule fields (Vanreusel et al., 2016).

296 The species accumulation curves showed that no asymptote was reached not at seamounts, nor at  
297 nodule fields. Consequently, longer transect lengths might be necessary to representatively quantify  
298 and assess megafauna density and diversity (Simon-Llédó et al., 2019). In addition, for a first in-  
299 depth description and assessment of seamount fauna composition, one video transect is insufficient  
300 to describe the diversity and shifts in faunal assemblages of the surveyed seamounts. Rather, an  
301 ampler imaging strategy should be developed, with a minimum transect length exceeding 1000ms  
302 (Simon-Llédó et al., 2019) and replicate transects carried out on different faces of the seamount, on  
303 slopes with varying degree of exposure to currents and different substrate types. Wider depth  
304 ranges should be taken into account as well. Despite its limitations, this study grants first insights in  
305 the seamount inhabiting megafauna of the eastern CCZ and an important first comparison with  
306 nodule fauna.

#### 307 4.2. Faunal (dis)similarities between seamounts and nodule fields

308 Seamounts were shown to share fauna with surrounding habitats (Clark et al., 2010) and potentially  
309 serve as source populations for neighbouring environments (McClain et al., 2009). While generally  
310 few species seemed restricted to seamounts only (Clark et al., 2010), in this study, morphospecies  
311 revealed to be quite different between seamounts and nodule fields with little overlap between  
312 both. Despite the high degree of variation observed among all the video transects, these grouped  
313 into two distinctly separate clusters, separating nodule from seamount transects. The few  
314 overlapping morphospecies did occur in different densities in each ecosystem, implying a different  
315 role or importance in the ecological community and its functioning.

316 Taxa contributing to the differences between the two ecosystems are discussed here. Ophiuroids  
317 were more abundant on the nodule fields. Asteroids and echinoids (with exception of one very  
318 abundant morphospecies at the nodule fields) were both more abundant and diverse on the  
319 seamounts. Both ophiuroid and echinoids were shown to be present in both nodule-rich and -free  
320 areas, though their densities decreased more than 50% comparing the former to the latter  
321 (Vanreusel et al., 2016). Despite the abundance of hard substrata at seamounts, this was true for the  
322 ophiuroid densities observed here (>50% decrease from nodule fields to seamounts), but not for the  
323 echinoids, where differences in overall density between ecosystems were less pronounced.



324 Ophiuroids did not show high levels of richness or endemism on seamounts (O'Hara, 2007). Same  
325 ophiuroid morphospecies were present at seamounts and nodule fields but in very different  
326 abundances and they showed preference for different substrata (at nodule fields on soft sediment  
327 (morphospecies 6), at seamounts on hard substrata (morphospecies 5)), which appeared to  
328 correspond to different lifestyles, feeding behaviour and corresponding dietary specialisations  
329 (Persons and Gage, 1984). Ophiuroids were often observed in association with xenophyophores at  
330 nodule fields (Amon et al., 2016) and at east Pacific seamounts (Levin et al., 1986), though no such  
331 associations were observed on the seamounts studied.

332 Holothuroid composition varied distinctly between nodule fields and seamounts with more families  
333 being observed at the latter. Many holothurians feed on the upper layers of the soft-bottom  
334 sediment (Bluhm and Gebruk, 1999), suggesting that their numbers would decrease when there is  
335 less sediment available. However, at the seamounts, many holothurians were observed on top of  
336 rocks, possibly reflecting different feeding strategies and explaining the observations of different  
337 morphospecies. Geographical variations, different bottom topography, differences in nodule  
338 coverages and sizes and/or an uneven distribution of holothurians on the sea floor were thought to  
339 play a role in holothuroid community composition (Bluhm and Gebruk, 1999). On the other hand,  
340 variability in deep-sea holothuroid abundance was proposed to depend primarily on depth and  
341 distance from continents (see Billet, 1991 for a review).

342 Stalked organisms, such as Crinoidea and Hexactinellida (except for Amphidiscophora) rely on hard  
343 substrata for their attachment. Crinoidea were proportionally more abundant on seamounts,  
344 possibly because hard substrata were less limiting than in the nodule fields. Porifera proportions  
345 (stalked and non-stalked) varied among all analysed transects, revealing no particular trends in  
346 abundance. However, the species composition of deep-sea glass sponge communities from  
347 seamounts and polymetallic nodule fields was distinctly different. Polymetallic nodule field  
348 communities were predominated by widely-distributed genera such as *Caulophacus* and *Hyalonema*,  
349 whereas seamount communities seemed to have a rather unique composition represented by  
350 genera like *Saccocalyx*. Stalked organisms are considered being among the most vulnerable  
351 organisms when mining is concerned.

352 While alcyonacean and antipatharian corals were virtually absent from nodule-free areas (Vanreusel  
353 et al., 2016), this was not the case for the seamounts (although Alcyonacea densities were lower  
354 than on nodules). Depth difference added up to more than 3000m between Mann Borgese  
355 seamount (APEI3) and the nodule transects, which could explain the difference in Antipatharia which  
356 were more abundant at lower depths (Genin et al., 1986). The antipatharian and alcyonacean  
357 morphospecies that were abundant on the seamounts did not occur on the nodule fields and vice  
358 versa, with exception of *Callozostron cf. bayeri* which was present at the nodule fields but in very  
359 low densities (1/10 of those observed at seamounts). Additional presence of Pennatulacea, which  
360 were virtually absent from the nodule field transects, resulted in a completely distinct coral  
361 community for both ecosystems.

362 Actiniaria were more abundant on nodule fields. It was denominated the second most common  
363 group at CCZ, after the xenophyophores (Kamenskaya et al., 2015). Depending on the species and  
364 feeding strategy, the ratio hard/soft substrata and their preference for either one could play a role.  
365 Since morphospecies were distinct between seamounts and nodule fields, their role in the



366 respective communities are likely to differ as well. Combinations of deposit feeding and predatory  
367 behaviour in Actiniaria have been observed, as well as burrowing activity, preference for attachment  
368 to hard substrata and exposure to currents (Durden et al., 2015a; Lampitt and Paterson, 1987;  
369 Riemann-Zürneck, 1998).

370 Some taxa were only observed on seamounts, while they were also known to occur on nodule fields,  
371 be it in low densities. The exception were the Scleractinia, which were absent at nodule fields but  
372 quite common on seamounts (e.g. this study, Baco, 2007). Contrastingly, Enteropneusta were  
373 observed previously at CCZ nodule fields though observations were rather rare (Tilot, 2006). They  
374 appeared more abundant at the nodule fields of the Deep Peru Basin (DISCOL area), though a wide  
375 range in abundances was displayed there as well (Bluhm, 2001).

376 Explanation for the discrepancies observed here in faunal composition and low degree of  
377 morphospecies overlap between seamount and nodule fields can be multiple. For one, nodules may  
378 not be considered a plain hard substratum, with their metal composition, microbial colonisation and  
379 the nodule/sediment interface influencing the epi- and associated megafaunal composition. The  
380 possibility of a specific deep-sea faunal community that tolerates or benefits from manganese  
381 substrata has been previously proposed (Mullineaux, 1988). The comparison between seamounts  
382 and nodule fields as two neighbouring hard-substrata ecosystems also entailed a comparison  
383 between depth gradients and possible thresholds (>4000m for nodule fields and 1500 <x <4000m for  
384 seamounts). Related to this is the steepness of the seamount slope and its current exposure playing  
385 a role in the faunal colonisation (Genin et al., 1986; Rappaport et al., 1997). Other studies showed  
386 that habitat heterogeneity increased megafaunal diversity at seamounts (Raymore, 1982) and  
387 elsewhere, such as abyssal plains (Lapointe and Bourget, 1999; Durden et al., 2015b, Leitner et al.,  
388 2017, Simon-Llédo et al., 2019). Within this perspective the ratio hard/soft substrata or amount of  
389 hard substrata available could play a role as well.

## 390 5. Conclusions

391 Based on our current knowledge; seamounts appear inadequate as refuge areas to help maintain  
392 nodule biodiversity. In order to conclusively exclude seamount habitats as a refuge for nodule fauna,  
393 a more comprehensive sampling should be carried out. The sampling strategy wielded in this study  
394 lacked replicates, uniformity and was limited in sample size. Seamount bases should be taken into  
395 consideration as well as they can be characterised by distinctly different assemblages than the  
396 summits and they occur at a depth range more similar to nodule fields.

397 While their role as refuge area for nodule field fauna is currently debatable, the possible uniqueness  
398 of the seamount habitat and its inhabiting fauna implies that seamounts need to be included in  
399 management plans for the conservation of the biodiversity and ecosystems of the CCZ.

## 400 Author Contributions

401 DC, PAR, SPR, DK analysed the images. DC analysed the data. PMA, PAR, AC conceptualised and  
402 carried out the sampling. All authors contributed to the redaction of the manuscript.

## 403 Data Availability

404 Data sets are made available through OSIS-Kiel data portal, BIIGLE and PANGAEA.



405 Competing interest

406 The authors declare that they have no conflict of interest

407 Acknowledgments

408 We thank the crew of SO239 and GEOMAR for their support in acquiring the images used in this  
409 article. The EcoResponse cruise with RV Sonne was financed by the German Ministry of Education  
410 and Science BMBF as a contribution to the European project JPI-Oceans “Ecological Aspects of Deep-  
411 Sea Mining”. This study had the support of PO AÇORES 2020 project Acores-01-0145-Feder-  
412 000054\_RECO and of Fundação para a Ciência e Tecnologia (FCT), through the strategic projects  
413 UID/MAR/04292/2013 granted to MARE. The authors acknowledge funding from the JPI Oceans—  
414 Ecological Aspects of Deep Sea Mining project by Fundação para a Ciência e Tecnologia de Portugal  
415 and the European Union Seventh Framework Programme (FP7/2007–2013) under the MIDAS  
416 project, grant agreement n° 603418. DC is supported by a post-doctoral scholarship  
417 (SFRH/BPD/110278/2015) from FCT. PAR was funded by the Portuguese Foundation for Science and  
418 Technology (FCT), through a postdoctoral grant (ref. SFRH/BPD/69232/2010) funded through QREN  
419 and COMPETE. SPR is supported by FCT in the scope of the “CEEC Individual 2017” contract  
420 (CEECIND/00758/2017) and CESAM funds (UID/AMB/50017/2019) through FCT/MCTES. AC is  
421 supported by Program Investigador (IF/00029/2014/CP1230/CT0002) from FCT. PMA acknowledges  
422 funding from BMBF contract 03 F0707E. Pictures were provided by GEOMAR (Kiel).  
423

424 References

- 425 Amon, D. J., Ziegler, A. F., Dahlgren, T. G., Glover, A. G., Goineau, A., Gooday, A. J., Wiklund, H.,  
426 and Smith, C. R.: Insights into the abundance and diversity of abyssal megafauna in a  
427 polymetallic-nodule region in the eastern Clarion-Clipperton Zone. *Sci. Rep.*, 6(1), 30492.  
428 <https://doi.org/10.1038/srep30492>, 2016
- 429 Beaulieu, S. E.: Colonization of habitat islands in the deep sea: Recruitment to glass sponge stalks.  
430 *Deep-Sea Res Pt I*, 48(4), 1121–1137. [https://doi.org/10.1016/S0967-0637\(00\)00055-8](https://doi.org/10.1016/S0967-0637(00)00055-8), 2001
- 431 Bluhm, H.: Re-establishment of an abyssal megabenthic community after experimental physical  
432 disturbance of the seafloor. *Deep-Sea Res Pt II*, 48(17–18), 3841–3868.  
433 [https://doi.org/10.1016/S0967-0645\(01\)00070-4](https://doi.org/10.1016/S0967-0645(01)00070-4), 2001
- 434 Bluhm, H., and Gebruk, A. V.: Holothuroidea (Echinodermata) of the Peru basin - ecological and  
435 taxonomic remarks based on underwater images. *Mar. Ecol.*, 20(2), 167–195.  
436 <https://doi.org/10.1046/j.1439-0485.1999.00072.x>, 1999
- 437 Boschen, R. E., Rowden, A. A., Clark, M. R., Barton, S., Pallentin, A., and Gardner, J.: Megabenthic  
438 assemblage structure on three New Zealand seamounts: implications for seafloor massive sulfide  
439 mining. *Mar. Ecol. Prog. Ser.*, 523, 1–14. <https://doi.org/10.3354/meps11239>, 2015
- 440 Clark, M. R., Rowden, A. A., Schlacher, T., Williams, A., Consalvey, M., Stocks, K. I., Rogers, A. D.,  
441 O’Hara, T. D., White, M., Shank, T. M., and Hall-Spencer, J. M.: The Ecology of Seamounts:  
442 Structure, Function, and Human Impacts. *Annu. Rev. Mar. Sci.*, 2(1), 253–278.  
443 <https://doi.org/10.1146/annurev-marine-120308-081109>, 2010
- 444 Clark, M. R., Schlacher, T. A., Rowden, A. A., K. Stocks, K. I., and Consalvey, M.: Science priorities  
445 for seamounts: research links to conservation and management. *PLoS One* 7(1): e29232., 2012
- 446 Durden, J. M., Bett, B. J., and Ruhl, H. A.: The hemisessile lifestyle and feeding strategies of *Iosactis*  
447 *vagabunda* (Actiniaria, Iosactiidae), a dominant megafaunal species of the Porcupine Abyssal  
448 Plain. *Deep-Sea Res Pt I* 102, 72–77. <https://doi.org/10.1016/j.dsr.2015.04.010>, 2015a
- 449 Durden, J. M., Bett, B. J., Jones, D. O. B., Huvenne, V. A. L., and Ruhl, H. A.: Abyssal hills - hidden  
450 source of increased habitat heterogeneity, benthic megafaunal biomass and diversity in the deep  
451 sea. *Prog. Oceanogr.*, 137, 209–218, <https://doi.org/10.1016/j.pocan.2015.06.006>, 2015b



- 452 Genin, A., Dayton, P. K., Lonsdale, P., and Spiess, F. N.: Corals on seamount peaks provide evidence  
453 of current acceleration over deep-sea topography. *Nature*, 322, 59–61, 1986
- 454 Kamenskaya, O. E., Gooday, A. J., Tendal, O. S., and Melnik, V. F.: Xenophyophores (Protista,  
455 Foraminifera) from the Clarion-Clipperton Fracture Zone with description of three new species.  
456 *Mar. Biodivers.*, 45(3), 581–593. <https://doi.org/10.1007/s12526-015-0330-z>, 2015
- 457 Kersken, D., Janussen, D., and Martinez Arbizu, P.: Deep-sea glass sponges (Hexactinellida) from  
458 polymetallic nodule fields in the Clarion-Clipperton Fracture Zone (CCFZ), northeastern  
459 Pacific: Part I – Amphidiscophora. *Mar. Biodivers.* 48, 545–573. [https://doi.org/10.1007/s10750-](https://doi.org/10.1007/s10750-017-3498-3)  
460 [017-3498-3](https://doi.org/10.1007/s10750-017-3498-3), 2018a
- 461 Kersken, D., Janussen, D., and Martinez Arbizu, P.: Deep-sea glass sponges (Hexactinellida) from  
462 polymetallic nodule fields in the Clarion-Clipperton Fracture Zone (CCFZ), northeastern  
463 Pacific: Part II—Hexasterophora. *Mar. Biodivers.* [https://doi.org/https://doi.org/10.1007/s12526-](https://doi.org/https://doi.org/10.1007/s12526-018-0880-y)  
464 [018-0880-y](https://doi.org/https://doi.org/10.1007/s12526-018-0880-y), 2018b
- 465 Lampitt, R. S., and Paterson, G. L. J.: The feeding behaviour of an abyssal sea anemone from in situ  
466 time lapse photographs and trawl samples. *Oceanol. Acta*, 10(4), 455–461, 1987
- 467 Lapointe, L., and Bourget, E.: Influence of substratum heterogeneity scales and complexity on a  
468 temperate epibenthic marine community. *Mar. Ecol. Prog. Ser.*, 189(2), 159–170.  
469 <https://doi.org/10.3354/meps189159>, 1999
- 470 Leitner, A. B., Neuheimer, A. B., Donlon, E., Smith, C. R., and Drazen, J. C.: Environmental and  
471 bathymetric influences on abyssal bait-attending communities of the Clarion Clipperton Zone.  
472 *Deep-Sea Res Pt I*, 125, 65–80. <https://doi.org/10.1016/j.dsr.2017.04.017>, 2017
- 473 Levin, L., DeMaster, D., McCann, L., and Thomas, C.: Effects of giant protozoans (class:  
474 Xenophyophorea) on deep-seamount benthos. *Mar. Ecol. Prog. Ser.*, 29, 99–104.  
475 <https://doi.org/10.3354/meps029099>, 1986
- 476 McClain, C. R., Lundsten, L., Barry, J., and DeVogelaere, A.: Assemblage structure, but not diversity  
477 or density, change with depth on a northeast Pacific seamount. *Mar. Ecol.*, 31, 14–25.  
478 <https://doi.org/10.1111/j.1439-0485.2010.00367.x>, 2010
- 479 McClain, C. R., Lundsten, L., Ream, M., Barry, J., and DeVogelaere, A.: Endemicity, biogeography,  
480 composition, and community structure on a Northeast Pacific seamount. *PLoS ONE*, 4(1).  
481 <https://doi.org/10.1371/journal.pone.0004141>, 2009
- 482 Mullineaux, L.S.: The role of settlement in structuring a hard-substratum community in the  
483 deep sea. *J. Exp. Mar. Biol. Ecol.* 120, 241–261, 1988
- 484 O'Hara, T. D.: Seamounts: Centres of endemism or species richness for ophiuroids? *Glob. Ecol.*  
485 *Biogeogr.*, 16(6), 720–732. <https://doi.org/10.1111/j.1466-8238.2007.00329.x>, 2007
- 486 Oksanen, J., Blanchet, G., Friendly, M., Kindt, R., Legendre, P., McGlinn, D., Minchin, P.R., O'Hara,  
487 R.B., Simpson, G.L., Solymos, P., Stevens, M.H.H., Szoecs, E., and Wagner, H.: vegan:  
488 Community Ecology Package. R package version 2.5-2. [https://CRAN.R-](https://CRAN.R-project.org/package=vegan)  
489 [project.org/package=vegan](https://CRAN.R-project.org/package=vegan), 2018
- 490 Rappaport, Y., Naar, D. F., Barton, C. C., Liu, Z. J., and Hey, R. N.: Morphology and distribution of  
491 seamounts surrounding Easter Island. *J. Geophys. Res.*, 102(B11), 24713.  
492 <https://doi.org/10.1029/97JB01634>, 1997
- 493 R Core Team: R: A language and environment for statistical computing. R Foundation for Statistical  
494 Computing, Vienna, Austria. URL <https://www.R-project.org/>, 2018
- 495 Riemann-Zürneck, K.: How sessile are sea anemones? A review of free-living forms in the Actiniaria  
496 (Cnidaria: Anthozoa). *Mar. Ecol.*, 19(4), 247–261. [https://doi.org/10.1111/j.1439-](https://doi.org/10.1111/j.1439-0485.1998.tb00466.x)  
497 [0485.1998.tb00466.x](https://doi.org/10.1111/j.1439-0485.1998.tb00466.x), 1998
- 498 Rogers, A.D.: The Biology of Seamounts: 25 years on. *Adv. Mar. Biol.* 79, 137–224,  
499 <https://doi.org/10.1016/bs.amb.2018.06.001>, 2018
- 500 Simon-Iledó, E., Bett, B. J., Huvenne, V. A. I., Schoening, T., Benoist, N. M. A., Je, R. M., Durden,  
501 J.M., and Jones, D. O. B.: Megafaunal variation in the abyssal landscape of the Clarion  
502 Clipperton Zone, *Progr. Oceanogr.* 170, 119–133. <https://doi.org/10.1016/j.pocean.2018.11.003>,  
503 2019
- 504 Tilot, V., Ormond, R., Moreno Navas, J., and Catalá, T. S.: The Benthic Megafaunal Assemblages of



505 the CCZ (Eastern Pacific) and an Approach to their Management in the Face of Threatened  
506 Anthropogenic Impacts. *Front Mar Sci.*, 5, 1–25. <https://doi.org/10.3389/fmars.2018.00007>,  
507 2018  
508 Vanreusel, A., Hilario, A., Ribeiro, P. A., Menot, L., and Arbizu, P. M.: Threatened by mining,  
509 polymetallic nodules are required to preserve abyssal epifauna. *Sci. Rep.*, 6(1), 26808.  
510 <https://doi.org/10.1038/srep26808>, 2016  
511 Wedding, L. M., Friedlander, A. M., Kittinger, J. N., Watling, L., Gaines, S. D., Bennett, M., Hardy,  
512 S.M., and Smith, C.R.: From principles to practice : a spatial approach to systematic  
513 conservation planning in the deep sea. *Proc. R. Soc. B* 280: 20131684.  
514 <http://dx.doi.org/10.1098/rspb.2013.1684>, 2013  
515 Wessel, P., Sandwell, D., and Kim, S.-S.: The Global Seamount Census. *Oceanography* 23(1), 24–33,  
516 <https://doi.org/10.5670/oceanog.2010.60>, 2010  
517  
518  
519  
520  
521  
522  
523  
524  
525  
  
526  
  
527  
  
528  
  
529  
  
530  
  
531  
  
532  
  
533  
  
534  
  
535  
  
536  
  
537  
  
538  
  
539  
  
540  
541  
542



543

## Tables

544

Table 1: Overview table on details of imagery transects analysed in the Clarion-Clipperton license areas. Video duration includes time spent sampling. Transect lengths do not include parts visualising ancient disturbance tracks.

545

Station/Dive	License Area	Seamount (SM) or Nodule field (NF)	Depth (m)	Video duration	Transect length	# obs/dive	# obs /100m
SQ239_29_ROV02	BGR	SM: Rüppell	3000-2500	7h47	1250m	414	33.1
SQ239_41_ROV03	BGR	NF	4080-4110	6h32	1590m	1023	64.3
SQ239_54_ROV04	BGR	SM: Senckenberg	3350-2850	8h45	2500m	853	34.1
SQ239_131_ROV08	GSR	NF	4470-4480	7h35	710m	486	68.5
SQ239_135_ROV09	GSR	SM: Heip	3900-3550	7h35	1000m	365	36.5
SQ239_141_ROV10	GSR	NF	4455-4480	7h35	520m	464	89.2
SQ239_189_ROV13	APEI 3	NF	4890-4930	9h01	1790m	136	7.6
SQ239_200_ROV14	APEI 3	NF	4650-4670	9h19	1490m	184	12.2
SQ239_212_ROV15	APEI 3	Mann Borgese	1850-1650	6h25	900m	366	40.7

546

547

548

549

550

551

552

553

554

555

556

557

558

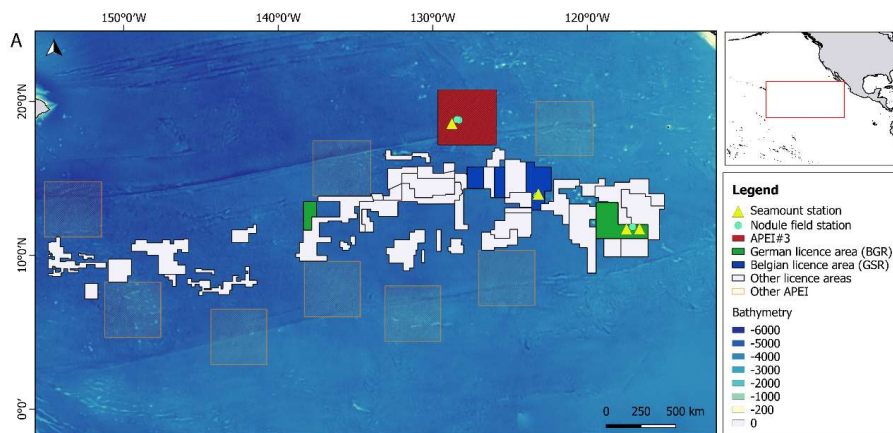
559

560



561

## Figures



562

563

Fig. 1. Location of the Clarion-Clipperton Fracture zone in the equatorial eastern Pacific Ocean featuring the contract areas from the International Seabed Authority (ISA) and the positions of the sampled areas (seamounts and nodule fields). Information on transect length and depth gradients can be found in Table 1.

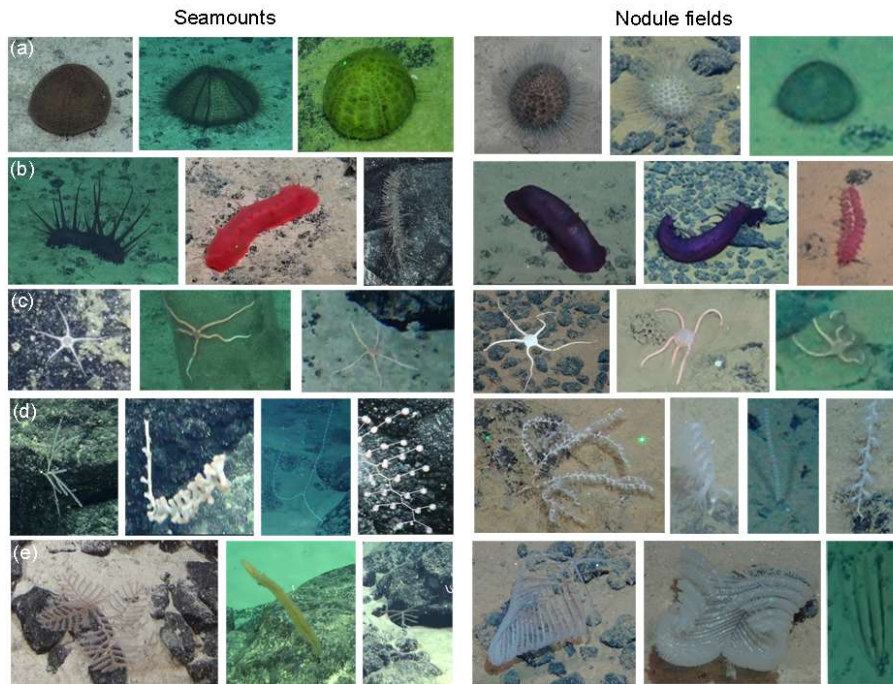
564

565

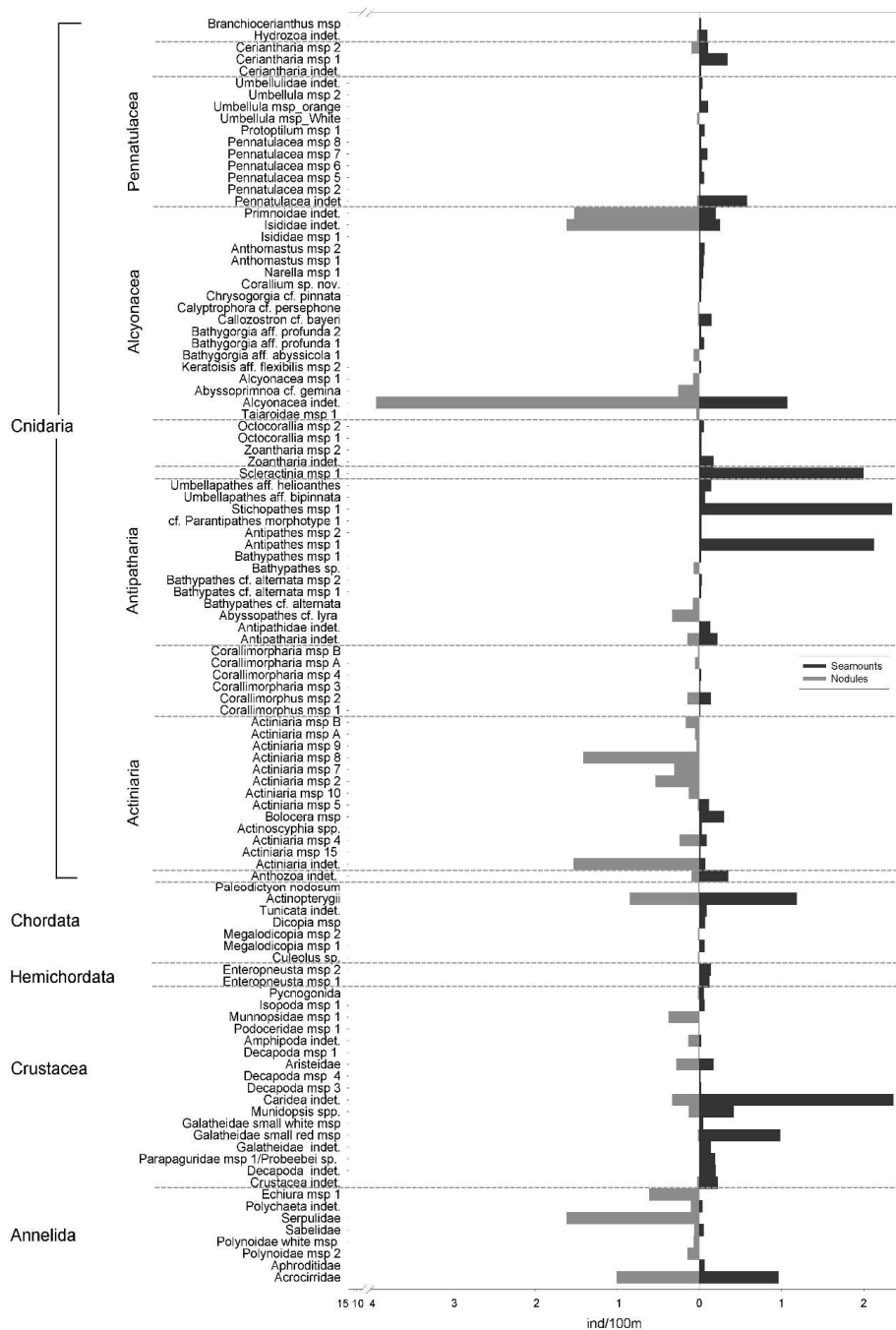
566

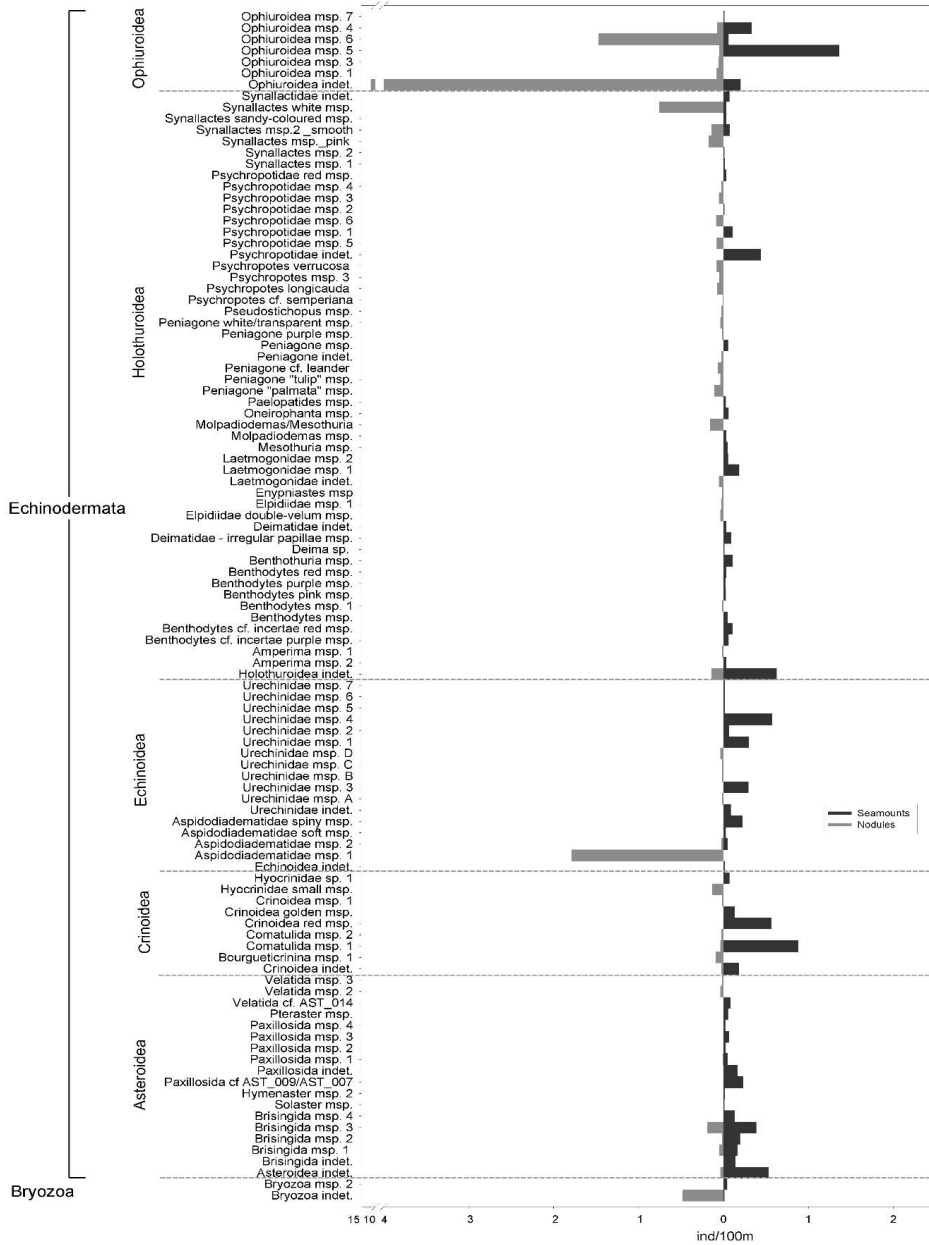
567

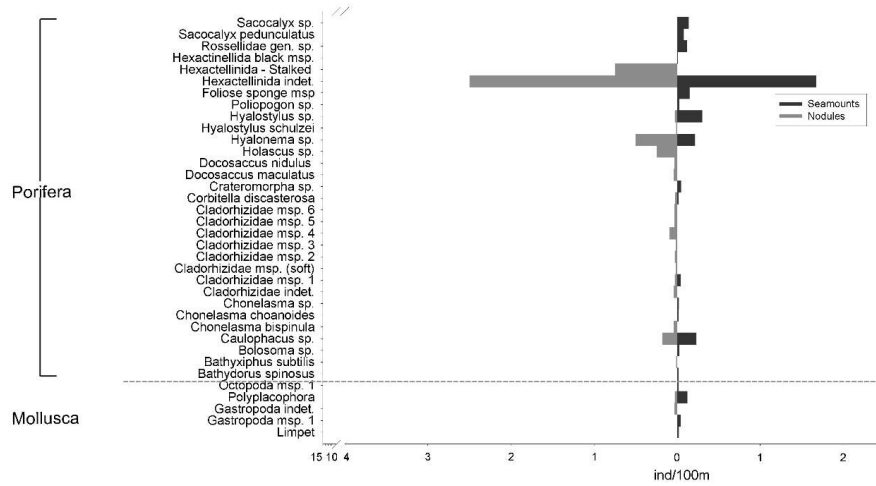
568



569  
570 Fig. 2. Some examples of different morphospecies at seamounts and nodule fields in the CCZ.  
571 Selected taxa were (a) Echinoidea, (b) Holothuroidea, (c) Ophiuroidea, (d) Alcyonacea, (e)  
572 Antipatharia. Copyright: SO239, ROV Kiel 6000, GEOMAR Helmholtz Centre for Ocean Research Kiel



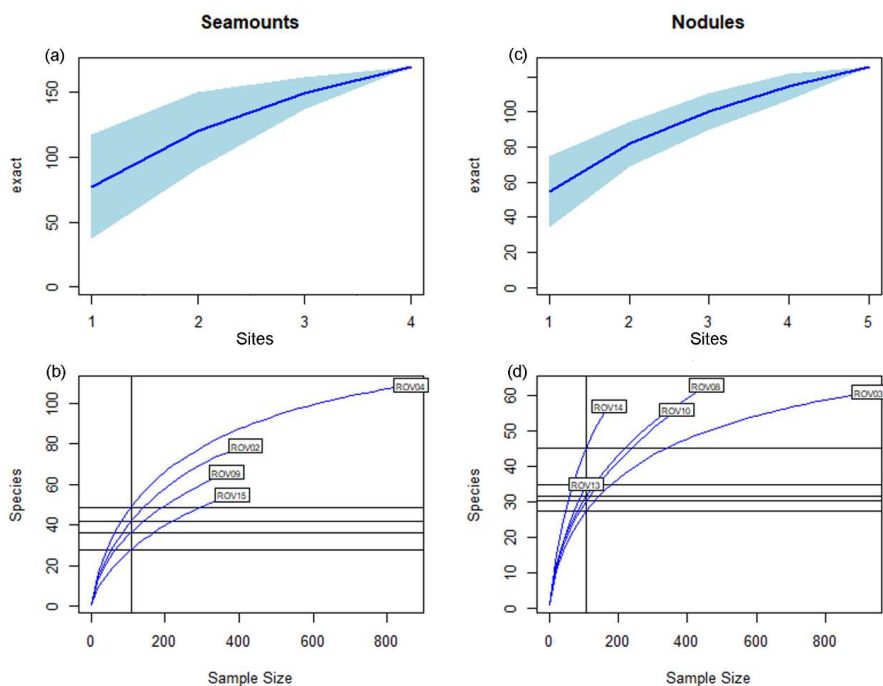




575  
 576 Fig. 3. Back-to-back histogram comparing average densities of morphospecies and taxa (ind/100m)  
 577 for seamount (#4) and nodule field (#5) video transects.

578

579

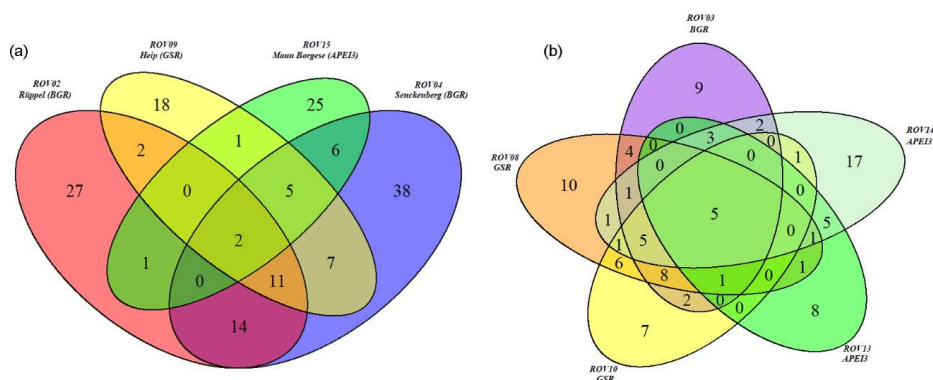


580 Fig. 4. Species accumulation (upper panel, a and c) and rarefaction curves (lower panel, b and d) for  
581 the seamount (#4) and nodule field (#5) transects. Seamount dives: ROV02= Rüppel (BGR),  
582 ROV04=Senckenberg (BGR), ROV09=Heip (GSR), ROV15=Mann Borgese (APEI3) in the lower left  
583 panel (b). Nodule field dives: ROV03 was carried out in the BGR area, ROV08 and 10 in the GSR area  
584 and ROV13 and 14 in the APEI3, presented in the lower right panel (d).  
585

586

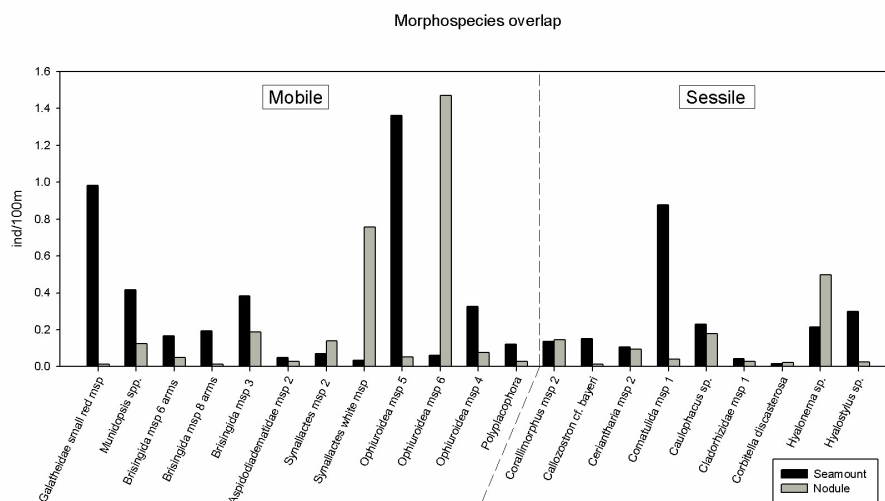
587

588



589  
 590 Fig. 5. A Venn diagram showing the unique and shared morphospecies among seamount video  
 591 transects. Values are relative due to different transect lengths and differences in richness. Left panel  
 592 (a) features seamount transects and the right panel features the 5 nodule field transects. Colour  
 593 codes were adapted among panels, with APEI3 nodule transects in green, related to Mann Borgese  
 594 seamount transect. BGR (ROV03) transect was purple in correspondence to BGR seamount transects  
 595 (red=Rüppel and blue=Senckenberg). GSR transects (ROV08 and 09) were shades of yellow.

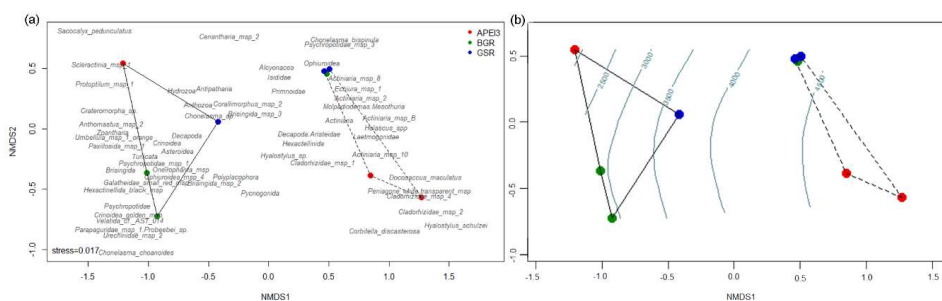
596  
 597  
 598  
 599  
 600  
 601  
 602



603

604 Fig. 6. Morphospecies overlap and average density (ind/100m) between seamounts and nodule  
 605 fields

606



607

608 Fig. 7. nMDS-plot with faunal densities and Bray-Curtis distances. Left panel (a) presents the  
 609 grouping of the video transects based on their faunal composition and right panel (b) features the  
 610 same plot but with depth as a vector fitting. Dotted lines group the nodule transects while the full  
 611 line groups the seamount transects.

612

613

614

615

616



617

## Appendix

618 Table A1. Overview of all taxa densities (ind./100m) and number of morphospecies (msp.) observed  
619 within each video transect. Msp. numbers represent often minimum numbers and are indicative.  
620 Higher taxa are in bold. \* indicates taxa left out of the statistical analyses due to lack of  
621 representativity. Indets were organisms impossible to attribute to a lower taxonomic group.  
622 ROV02=Rüppel, ROV04=Senkcnberg, ROV09=Heip, ROV15=Mann Borgese





